An Overview of the Physical Insight and the Various Performance Metrics of Fading Channels in Wireless Communication Systems

K.P. Peppas[1], H.E. Nistazakis[2] and G.S. Tombras[3]
[1]*National Center Of Scientific Research "Demokritos"*
[2,3]*Department of Electronics, Computers, Telecommunications and Control,*
Faculty of Physics
National and Kapodistrian University of Athens
Greece

1. Introduction

In this chapter, we discuss on the physical insight and the various performance metrics of the wireless channels environment in today's communications schemes. The availability and reliability of such channels is closely related to the transmitted-received signal fading conditions, a well known electromagnetic wave mitigation phenomenon due either to multipath wave propagation or to shadowing from physical or man-made obstacles that affect wave propagation. In this respect, we first examine the various types of fading that the propagated signals may experience, being the multi-path induced or fast fading and the shadow or slow fading, as well as flat fading and frequency selective fading. Then, we present the methodologies that have been suggested for evaluating fading channels and rely on different statistical distributions of the corresponding signal amplitude and phase variations. Such distributions have been concluded from the study of the physical phenomena and laws that govern wave propagation over different areas and under various conditions and most of them have been experimentally studied. Following the above, we consider the most of the main mathematical models that have been proposed and validated over time in describing the fading channels characteristics and concentrate on three important performance metrics being the average, or ergodic, capacity, the outage probability and the average bit error probability. Finally, by considering each of those fading channel models, we discuss their analytic convenience and accuracy with respect to the physical conditions implied.

2. Basic characteristics of fading channels

The propagation of energy in a mobile radio environment is characterized by various effects including multi-path fading and shadowing. Such phenomena result in variations of the channel strength over both time and frequency, thus impairing the performance of wireless receivers. The above mentioned variations can be roughly classified into two categories:

- *Large Scale Fading*: This type of fading is due to path loss and shadowing. Path loss is the attenuation of the electromagnetic wave radiated by the transmitter as it propagates

through space. It is noted that path loss is a major component in the analysis and design of the link budget of a telecommunication system. Shadowing occurs where a large obstacle between the transmitter and receiver obscures the main signal path between the transmitter and the receiver. Such obstacles attenuate signal power through absorption, reflection, scattering, and diffraction; when the attenuation is very strong, the signal is blocked.

- *Small Scale Fading*: In a wireless communication environment, the propagation of energy is characterized by waves that interact with physical obstacles via mechanisms such as reflection, scattering, diffraction and absorption. This interaction, results in the generation of a continuous distribution of partial waves (Braun & Dersch, 1991; Yacoub, 2007b). Each wave experiences differences in attenuation, delay and phase shift in accordance with the physical properties of the surface. The propagated signal arrives at the receiver through multiple paths, resulting in a rapidly fading combined signal. This phenomenon can have a constructive or destructive impact on the receiving signal, amplifying or attenuating the signal power seen at the receiver. Small Scale Fading typically occurs over very short distances, on the order of the carrier wavelength (Goldsmith, 2005).

Fading phenomena can also be classified to slow and fast fading. Such a classification is useful for the mathematical modeling of fading channels as well as for the performance assessment of communication systems operating over fading channels. The terms "slow" and "fast" refer to the rate at which the magnitude and phase of the received signal varies with respect to the channel changes. This classification is closely related to the coherence time T_c of the channel. The coherence time is a measure of the minimum time required for the magnitude change of the channel to become uncorrelated from its previous value, or equivalently, the period of time after which the correlation function of two samples of the channel response taken at the same frequency but different time instants drops below a predefined threshold. The coherence time is also related to the channel Doppler spread f_d as

$$T_c \simeq 1/f_d. \tag{1}$$

A wireless channel is called slow fading, when the coherence time of the channel, T_c, is large relative to the delay requirement of a specific application. In slow fading, the amplitude and phase change imposed by the channel can be considered roughly constant over the period of use. On the other hand, fast fading occurs when the coherence time of the channel, T_c is small relative to the delay requirement of the application (Simon & Alouini, 2005). In fast fading, the amplitude and phase change imposed by the channel varies considerably over the period of use. It should be noted that in a fast fading channel, coded symbols can be transmitted over multiple fades of the channel while in slow fading they cannot. Therefore, the characterization of a fading channel as slow or fast does not depend only on the environment but also on the application and the demanding bit rate (Tse & Viswanath, 2005). In practice, the characterization of a channel as fast or slow fading, depends strongly on the bit rate of the link. More specifically, as data rates increase, wireless communication channels become better described as slow fading. On the other hand, as the data rates decrease, the channel is better described as a fast fading one (Belmonte & Kahn, 2009).

Frequency selectivity is another important characteristic of fading channels. In flat fading, the coherence bandwidth of the channel is larger than the bandwidth of the signal. Therefore, all spectral components of the transmitted signal will experience the same magnitude of fading. This is the case for narrow-band systems, in which the transmitted signal bandwidth is much smaller than the channel's coherence bandwidth f_c. The coherence bandwidth is defined

as the approximate maximum frequency interval over which two frequencies of a signal are likely to experience correlated amplitude fading and measures the frequency range over which the fading process is correlated. The coherence bandwidth is related to the maximum delay spread τ_{max} by

$$f_c \simeq 1/\tau_{max} \tag{2}$$

On the other hand, in frequency selective fading the spectral components of the transmitted signal are affected by different amplitude gains and phase shifts. This is the case for wide-band systems in which the channel's coherence bandwidth is smaller than the transmitted signal bandwidth.

3. Statistical modeling of flat fading channels

Depending on the nature of the propagation environment, the statistics of the mobile radio signal are well described by a great number of distributions available in the open technical literature. The short-term signal variation is described by several distributions, such as the Rayleigh, Rice (Nakagami-n), Nakagami-m, Hoyt (Nakagami-q), and Weibull distributions. The derivation of these well-known fading distributions is based on the assumption of a homogeneous diffuse scattering field, resulting from randomly distributed point scatterers. The assumption is however an approximation since the surfaces are spatially correlated in a realistic propagation environment (Braun & Dersch, 1991; Yacoub, 2007b). To address such non-homogeneities of the propagation medium more generic distributions have been proposed such as the generalized gamma, the κ-μ and the η-μ distributions.

Moreover, in addition to multi-path fading, the quality of the received signal is also affected by shadowing. The statistics of the path gain due to shadowing can be appropriately described by the log-normal distribution. In some environments, however, such as congested downtown areas and land-mobile satellite systems with urban shadowing, the receiver should react to the instantaneous composite multipath/shadow faded signal. In these cases, analysis of the channel model must take into account both multi-path and shadow fading.

In this section, we present an overview of the most popular distributions used for statistical fading models. Throughout this presentation, a narrow-band digital receiver is assumed. The fading amplitude at the input of the receiver, R is a random variable (RV) with mean-square value $\Omega = \mathbb{E}\langle R^2 \rangle$ with $\mathbb{E}\langle \cdot \rangle$ denoting expectation. We also define the probability density function (PDF) of R, $f_R(r)$ which depends on the nature of the propagation environment. The equivalent baseband received signal can be expressed as $z = sR + n$, where s is the transmitted symbol, and n is the additive white gaussian noise (AWGN) having one-sided power spectral density N_0 Watts/Hz. Typically, n is assumed to be statistically independent of R. The instantaneous signal-to-noise (SNR) per received symbol is $\gamma = R^2 E_s/N_0$, where $E_s = \mathbb{E}\langle |s|^2 \rangle$ is the energy per symbol. The corresponding average SNR per symbol is $\overline{\gamma} = \Omega E_s/N_0$. Performing a simple RV transformation, the PDF of γ is obtained as

$$f_\gamma(\gamma) = \frac{f_R\left(\sqrt{\frac{\Omega\gamma}{\overline{\gamma}}}\right)}{2\sqrt{\frac{\overline{\gamma}\gamma}{\Omega}}} \tag{3}$$

Finally, we define the moment generating function (MGF) $\mathcal{M}_\gamma(s)$ of γ as

$$\mathcal{M}_\gamma(s) \triangleq \mathbb{E}\langle \exp(-s\gamma) \rangle = \int_0^\infty \exp(-s\gamma) f_\gamma(\gamma) \mathrm{d}\gamma. \tag{4}$$

In the following, the most commonly used fading distributions will be presented with respect to their PDFs and MGFs.

3.1 The Rayleigh fading model

The Rayleigh fading model agrees very well with experimental data when there are many objects in the environment that scatter the radio signal before it arrives at the receiver. It can also be applied to the propagation through the troposphere and ionosphere (Basu et al., 1987; James & Wells, 1955; Sugar, 1955) and to ship-to-ship radio links (Staley et al., 1996). According to the central limit theorem, if there is sufficiently much scatter, the channel impulse response will be well-modelled as a zero mean complex Gaussian process. In this case, the envelope of the channel impulse response will be Rayleigh distributed whereas the phase uniformly distributed between 0 and 2π radians. The probability density function of the channel fading amplitude R is given as

$$f_R(r) = \frac{2r}{\Omega} \exp\left(-\frac{r^2}{\Omega}\right), r \geq 0. \tag{5}$$

Using (3), the PDF of the equivalent instantaneous SNR per symbol, γ is given by

$$f_\gamma(\gamma) = \frac{1}{\overline{\gamma}} \exp\left(-\frac{\gamma}{\overline{\gamma}}\right), \gamma \geq 0. \tag{6}$$

As it can be observed, γ is exponentially distributed with parameter $1/\overline{\gamma}$. Finally, the MGF of γ is expressed in closed-form as follows

$$\mathcal{M}_\gamma(s) = \frac{1}{1 + s\overline{\gamma}}. \tag{7}$$

3.2 The Rice fading model

The Rice fading model, also known as the Nakagami-n fading model, arises when there is a strong line-of-sight (LOS) component and many weaker components in the received signal (Rice, 1948). This model is common in micro-cellular urban and suburban land-mobile systems, pico-cellular indoor, satellite and ship-to-ship radio links (Bultitude et al., 1989; Munro, 1963; Rappaport & McGillem, 1989; Shaft, 1974). The probability distribution for the envelope of the received signal is given by:

$$f_R(r) = \frac{2(1+n^2)e^{-n^2}r}{\Omega} \exp\left[-\frac{(1+n^2)r^2}{\Omega}\right] I_0\left(2nr\sqrt{\frac{1+n^2}{\Omega}}\right), r \geq 0 \tag{8}$$

where $0 \leq n < \infty$ is the fading parameter and $I_0(\cdot)$ is the modified Bessel function of the first kind and zero order (Gradshteyn & Ryzhik, 2000b, Eq. (8.406)). The quantity $K = n^2$ is called the Rice factor. Note that setting $K = 0$ transforms this model into the Rayleigh fading model and setting $K = \infty$ would transform it into a simple AWGN model with no fading.
Using (3), the PDF of γ is given by

$$f_\gamma(\gamma) = \frac{(1+n^2)e^{-n^2}}{\overline{\gamma}} \exp\left[-\frac{(1+n^2)\gamma}{\overline{\gamma}}\right] I_0\left(2n\sqrt{\frac{(1+n^2)\gamma}{\overline{\gamma}}}\right), \gamma \geq 0. \tag{9}$$

An Overview of the Physical Insight and the
Various Performance Metrics of Fading Channels in Wireless Communication Systems

7

As it can be observed, γ follows a non-central chi-square distribution. Finally, the MGF of γ is expressed in closed-form as follows

$$\mathcal{M}_\gamma(s) = \frac{1+n^2}{1+n^2+s\overline{\gamma}} \exp\left(-\frac{n^2 s\overline{\gamma}}{1+n^2+s\overline{\gamma}}\right). \tag{10}$$

3.3 The Hoyt fading model

The Hoyt fading model, also known as the Nakagami-q fading model (Hoyt, 1947), is common in satellite links subject to strong ionospheric scintillation (Bischoff & Chytil, 1969; Chytil, 1967). The probability distribution for the envelope of the received signal is given by:

$$f_R(r) = \frac{r(1+q^2)}{q\Omega} \exp\left[-\frac{(1+q^2)^2 r^2}{4q^2\Omega}\right] I_0\left(\frac{(1-q^4)r^2}{4q^2\Omega}\right), r \geq 0. \tag{11}$$

where $0 \leq q \leq 1$ is the fading parameter.
The PDF of γ is given by

$$f_\gamma(\gamma) = \frac{(1+q^2)}{2q\overline{\gamma}} \exp\left[-\frac{(1+q^2)^2\gamma}{4q^2\overline{\gamma}}\right] I_0\left(\frac{(1-q^4)\gamma}{4q^2\overline{\gamma}}\right), \gamma \geq 0. \tag{12}$$

Moreover, the MGF of γ is expressed in closed form as

$$\mathcal{M}_\gamma(s) = \left[1 + 2s\overline{\gamma} + \frac{(2s\overline{\gamma})^2 q^2}{(1+q^2)^2}\right]^{-1/2}. \tag{13}$$

3.4 The Weibull fading model

The Weibull fading, is a simple and flexible statistical model of fading used in wireless communications and based on the Weibull distribution. Empirical studies have shown it to be an effective model in both indoor and outdoor environments (Bertoni, 1988; Hashemi, 1993). Furthermore, this model has recently gained significant interest in the field of performance analysis of digital communications over fading channels (Karagiannidis et al., 2005; Sagias, Karagiannidis & Tombras, 2004; Sagias, Karagiannidis, Zogas, Mathiopoulos & Tombras, 2004; Sagias et al., 2003; Sagias & Tombras, 2007; Sagias, Zogas, Karagiannidis & Tombras, 2004; Zogas et al., 2005). The Weibull PDF is given by

$$f_R(r) = \frac{\beta}{(\Xi\Omega)^{\beta/2}} r^{\beta-1} \exp\left[-\left(\frac{r^2}{\Xi\Omega}\right)^{\beta/2}\right], r \geq 0. \tag{14}$$

where $\beta > 0$ is the fading parameter and $\Xi = 1/\Gamma(1+2/\beta)$, with $\Gamma(\cdot)$ being the Gamma function (Gradshteyn & Ryzhik, 2000b, Eq. (8.310/1)). For $\beta = 2$, (14) reduces to the Rayleigh fading model. The corresponding SNR per symbol has PDF given by

$$f_\gamma(\gamma) = \frac{\beta}{2(\Xi\overline{\gamma})^{\beta/2}} \gamma^{\beta/2-1} \exp\left[-\left(\frac{\gamma}{\Xi\overline{\gamma}}\right)^{\beta/2}\right], \gamma \geq 0. \tag{15}$$

One can observe that γ also follows a Weibull distribution with parameter $\beta/2$. For $\beta > 0$, the MGF of γ is expressed in closed form as (Yilmaz & Alouini, 2009)

$$\mathcal{M}_\gamma(s) = H_{1,1}^{1,1}\left[\frac{1}{\Xi\overline{\gamma}s}\left|\begin{matrix}(1,1)\\(1,2/\beta)\end{matrix}\right.\right]. \tag{16}$$

where $H_{p,q}^{m,n}(\cdot)$ is the H-Fox function (Cook, 1981). A computer program in Mathematica for the efficient implementation of the H-Fox function is given in (Yilmaz & Alouini, 2009, Appendix A). For the special case of $\beta = 2l/k$, where l, k are positive integers with $GCD(l,k) = 1$, the MGF can be expressed in terms of the more familiar Meijer-G function as (Sagias & Karagiannidis, 2005)

$$\mathcal{M}_\gamma(s) = \frac{\beta}{2} \frac{1}{(\Xi\overline{\gamma}s)^{\beta/2}} \frac{l^{\beta/2}\sqrt{k/l}}{(\sqrt{2\pi})^{k+l-2}} G_{l,k}^{k,l}\left[\frac{l^l/k^k}{(\Xi\overline{\gamma}s)^{k\beta/2}} \left|\begin{matrix} \Delta(l;1-\beta/2) \\ \Delta(k;0) \end{matrix}\right. \right] \tag{17}$$

where $G_{p,q}^{m,n}(\cdot)$ is the Meijer-G function (Prudnikov et al., 1986) and $\Delta(k;x) \triangleq \{x/k, (x+1)/k, \cdots, (x+k-1)/k\}$. Note that the Meijer-G function is available in popular software mathematical packages such as Maple or Mathematica. Moreover, from (Gradshteyn & Ryzhik, 2000b), the Meijer-G function can be written in terms of the more familiar generalized hypergeometric functions.

3.5 The Nakagami-m fading model

The Nakagami-m fading model is a purely empirical model and is not based on results derived from physical consideration of radio propagation. It also often gives the best fit to land-mobile and indoor-mobile propagation experimental data (Aulin, 1981; Braun & Dersch, 1991). Moreover, is mathematically tractable because it leads to closed form analytical expressions for important wireless communication systems performance metrics (Simon & Alouini, 2005). The distribution of the received signal's envelope is given by (Nakagami, 1960)

$$f_R(r) = \frac{2m^m r^{2m-1}}{\Omega^m \Gamma(m)} \exp\left(-\frac{mr^2}{\Omega}\right), r \geq 0 \tag{18}$$

where $1/2 \leq m \leq \infty$ is the fading parameter. parameter. For $m = 1$ the model reduces to the Rayleigh fading model whereas for $m = 1/2$ to the one sided gaussian distribution. The PDF of the SNR per symbol, γ is distributed according to a gamma distribution given by

$$f_\gamma(\gamma) = \frac{m^m \gamma^{m-1}}{\overline{\gamma}^m \Gamma(m)} \exp\left(-\frac{m\gamma}{\overline{\gamma}}\right), \gamma \geq 0 \tag{19}$$

It can easily be shown that the MGF of γ is given by

$$\mathcal{M}_\gamma(s) = \left(1 + \frac{s\overline{\gamma}}{m}\right)^{-m}. \tag{20}$$

3.6 Generalized fading models: The generalized-gamma, η-μ and κ-μ distributions

In many practical cases, situations are encountered for which no distributions seem to adequately fit experimental data, though one or another may yield a moderate fitting. Some researches (Stein, 1987) even question the use of the Nakagami-m distribution because its tail does not seem to yield a good fitting to experimental data, better fitting being found around the mean or median. Recently the so called generalized-gamma, η-μ and κ-μ distributions have been proposed as alternative generic fading models. These distributions fit well experimental data and include as special cases the well known distributions presented above.

An Overview of the Physical Insight and the
Various Performance Metrics of Fading Channels in Wireless Communication Systems

9

3.6.1 The generalized-gamma distribution

The generalized-gamma fading model, also known as the α-μ (Yacoub, 2007a) or Stacy fading model (Stacy, 1962), considers a signal composed of clusters of multi-path waves propagating in a non-homogeneous environment. Within any one cluster, the phases of the scattered waves are random and have similar delay times with delay-time spreads of different clusters being relatively large. The resulting envelope is obtained as a non-linear function of the modulus of the sum of the multipath components. The non-linearity is manifested in terms of a power parameter $\beta > 0$, such that the resulting signal intensity is obtained not simply as the modulus of the sum of the multipath components, but as this modulus to a certain given power (Yacoub, 2007a). The PDF of the fading envelope is given by

$$f_R(r) = \frac{\beta r^{m\beta-1}}{(\Omega\tau)^{m\beta/2}\Gamma(m)} \exp\left[-\left(\frac{r^2}{\Omega\tau}\right)^{\beta/2}\right], r \geq 0. \tag{21}$$

where $\beta > 0$ and $m > 1/2$ are parameters related to the fading severity and $\tau = \Gamma(m_i)/\Gamma(m_i + 2/\beta_i)$. This distribution is very generic as it includes the Rayleigh model ($\beta = 2, m = 1$), the Nakagami-m model ($\beta = 2$) and the Weibull model ($m = 1$). Moreover, for the limiting case ($\beta = 0, m = \infty$) it approaches the lognormal model. The PDF of the corresponding SNR is given by

$$f_\gamma(\gamma) = \frac{\beta\,\gamma^{m\beta/2-1}}{2\,\Gamma(m)\,(\tau\overline{\gamma})^{m\beta/2}} \exp\left[-\left(\frac{\gamma}{\tau\overline{\gamma}}\right)^{\beta/2}\right] \tag{22}$$

The MGF of γ is given by (Aalo et al., 2005; Yilmaz & Alouini, 2009)

$$\mathcal{M}_\gamma(s) = \frac{1}{\Gamma(m)} H_{1,1}^{1,1}\left[\frac{1}{\tau\overline{\gamma}s}\left|\begin{matrix}(1,1)\\(m,2/\beta)\end{matrix}\right.\right]. \tag{23}$$

For the special case of $\beta = 2l/k$, where l, k are positive integers with GCD$(l, k) = 1$, the MGF can be expressed in terms of the more familiar Meijer-G function as (Sagias & Mathiopoulos, 2005)

$$\mathcal{M}_\gamma(s) = \frac{\beta}{2\Gamma(m)} \frac{1}{(\tau\overline{\gamma}s)^{m\beta/2}} \frac{l^{m\beta/2}\sqrt{k/l}}{(\sqrt{2\pi})^{k+l-2}} G_{l,k}^{k,l}\left[\frac{l^l/k^k}{(\tau\overline{\gamma}s)^{k\beta/2}}\left|\begin{matrix}\Delta(l;1-\beta m/2)\\\Delta(k;0)\end{matrix}\right.\right] \tag{24}$$

3.6.2 The η-μ distribution

The η-μ fading model is a generic fading distribution that provides an improved modeling of small-scale variations of the fading signal in a *non-line-of-sight condition*. This model considers a signal composed of clusters of multipath waves propagating in a non-homogeneous environment. The phases of the scattered waves within any one cluster are random and they have similar delay times. It is also assumed that the delay-time spreads of different clusters are relatively large (Yacoub, 2007b). The η-μ distribution uses two parameters η and μ to accurately model a variety of fading environments. More specifically, it comprises both Hoyt ($\mu = 0.5$) and Nakagami-m ($\eta \rightarrow 0, \eta \rightarrow \infty, \eta \rightarrow \pm1$) distributions. Furthermore, it has been shown that it can accurately approximate the sum of independent non-identical Hoyt envelopes having arbitrary mean powers and arbitrary fading degrees (Filho & Yacoub, 2005). The η-μ fading model appears in two different formats: In Format 1, the in-phase and quadrature components of the fading signal within each cluster are assumed to be independent from each other and to have different powers, with the parameter $0 < \eta < \infty$ given by the ratio between them. In Format 2, $-1 < \eta < 1$ denotes the correlation between

the powers of the in-phase and quadrature scattered waves in each multi-path cluster. In both formats, the parameter $\mu > 0$ denotes the number of multi-path clusters. The PDF of the fading envelope R is given by

$$f_R(r) = \frac{4\sqrt{\pi}\mu^{\mu+\frac{1}{2}}h^\mu}{\Gamma(\mu)H^{\mu-\frac{1}{2}}}\left(\frac{r}{\hat{r}}\right)^{2\mu}\exp\left[-2\mu h\left(\frac{r}{\hat{r}}\right)^2\right]I_{\mu-\frac{1}{2}}\left(2\mu H\left(\frac{r}{\hat{r}}\right)^2\right) \tag{25}$$

where $\hat{r} = \sqrt{\Omega}$. The PDF of the corresponding average SNR per symbol γ is obtained as

$$f_\gamma(\gamma) = \frac{2\sqrt{\pi}\mu^{\mu+\frac{1}{2}}h^\mu}{\Gamma(\mu)H^{\mu-\frac{1}{2}}}\frac{\gamma^{\mu-\frac{1}{2}}}{\overline{\gamma}^{\mu+\frac{1}{2}}}\exp\left(-\frac{2\mu\gamma h}{\overline{\gamma}}\right)I_{\mu-\frac{1}{2}}\left(\frac{2\mu H\gamma}{\overline{\gamma}}\right). \tag{26}$$

In Format 1, $h = (2 + \eta^{-1} + \eta)/4$ and $H = (\eta^{-1} - \eta)/4$ whereas in Format 2, $h = 1/(1 - \eta^2)$ and $H = \eta/(1 - \eta^2)$. Finally, the MGF of γ, with the help of (Ermolova, 2008, Eq. (6)), (Peppas, Lazarakis et al., 2009, Eq. (2)) can be expressed as:

$$\mathcal{M}_\gamma(s) = (1 + As)^{-\mu}(1 + Bs)^{-\mu} \tag{27}$$

where $A = \frac{\overline{\gamma}}{2\mu(h-H)}$ and $B = \frac{\overline{\gamma}}{2\mu(h+H)}$.

3.6.3 The κ-μ distribution

The κ-μ fading model is a generic fading distribution that provides an improved modeling of small-scale variations of the fading signal in a *line-of-sight condition*. Similarly to the η-μ case, this model considers a signal composed of clusters of multipath waves propagating in a non-homogeneous environment. The phases of the scattered waves within any one cluster are random and they have similar delay times. It is also assumed that the delay-time spreads of different clusters are relatively large. The clusters of multipath waves are assumed to have scattered waves with identical powers, but within each cluster a dominant component is found (Yacoub, 2007b). As implied by its name, the κ-μ distribution uses two parameters κ and μ to accurately model a variety of fading enviromnents. More specifically, it comprises both Rice ($\mu = 1$) and Nakagami-m ($\kappa \to 0$) distributions. The parameter κ is defined as the ratio between the total power of the dominant components and the total power of the scattered waves, whereas the parameter μ denotes the number of multipath clusters. The PDF of the fading envelope R is given by

$$f_R(r) = \frac{2\mu(1+\kappa)^{\frac{\mu+1}{2}}}{\kappa^{\frac{\mu-1}{2}}\exp(\mu\kappa)}\left(\frac{r}{\hat{r}}\right)^\mu\exp\left[\mu(1+\kappa)\left(\frac{r}{\hat{r}}\right)^\mu\right]I_{\mu-1}\left(2\mu\sqrt{\kappa(1+\kappa)}\frac{r}{\hat{r}}\right) \tag{28}$$

where $\hat{r} = \sqrt{\Omega}$. The PDF of the corresponding average SNR per symbol, γ is easily obtained as

$$f_\gamma(\gamma) = \frac{\mu(1+\kappa)^{\frac{\mu+1}{2}}}{\kappa^{\frac{\mu-1}{2}}\exp(\mu\kappa)}\frac{\gamma^{\frac{\mu-1}{2}}}{\overline{\gamma}^{\frac{\mu+1}{2}}}\exp\left(-\frac{\mu(1+\kappa)\gamma}{\overline{\gamma}}\right)I_{\mu-1}\left(2\mu\sqrt{\frac{\kappa(1+\kappa)\gamma}{\overline{\gamma}}}\right) \tag{29}$$

Using (Ermolova, 2008) the MGF of γ is expressed in closed form as

$$\mathcal{M}_\gamma(s) = \frac{(1+\kappa)^\mu\mu^\mu}{[s\overline{\gamma} + (1+\kappa)\mu]^\mu}\exp\left(-\frac{\mu\kappa\overline{\gamma}s}{s\overline{\gamma} + \mu(1+\kappa)}\right) \tag{30}$$

3.7 Log-normal shadowing

The link quality of practical wireless communication systems is also affected by slow variation of the mean signal level due to shadowing. It is empirically confirmed that the log-normal distribution can accurately model the variation in received power in both outdoor and indoor radio propagation environments. The PDF of the instantaneous SNR per symbol γ is given by

$$f_\gamma(\gamma) = \frac{\xi}{\sqrt{2\pi}\sigma\gamma} \exp\left[-\frac{(10\log_{10}\gamma - \mu)^2}{2\sigma^2} \right] \tag{31}$$

where $\xi = 10/\ln 10 = 4.3429$, μ is the mean of $10\log_{10}\gamma$ expressed in dB and σ is the standard deviation of $10\log_{10}\gamma$, also in dB. The moment generating function of γ is given by

$$\mathcal{M}_\gamma(s) \simeq \frac{1}{\sqrt{\pi}} \sum_{n=1}^{N} w_{x_n} \exp\left(10^{(\sqrt{2}\sigma x_n + \mu)/10} s \right) \tag{32}$$

where x_n are the zeros of the N-order Hermite polynomial and w_{x_n} are the corresponding weight factors given by (Abramovitz & Stegun, 1964). Finally, it should be noted that the log-normal distribution is a very common and accurate model for wireless optical communication systems under weak atmospheric turbulence conditions (Kamalakis et al., 2006; Katsis et al., 2009; Laourine et al., 2007; Majumdar, 2005; Nistazakis, Tsiftsis & Tombras, 2009).

3.8 Generalized-K distribution

In a wireless propagation environment, multi-path fading and shadowing occur simultaneously in many practical cases. Such cases often appear in congested downtown areas with slow moving pedestrians and vehicles as well as in land-mobile satellite systems subject to vegetative and/or urban shadowing (Simon & Alouini, 2005). By averaging the signal power, which may follow one of the previously mentioned distributions, over the conditional density of the log-normally distributed mean signal power, various distributions may be obtained for modeling the composite environment, including the widely accepted Rayleigh- and Nakagami-log-normal (Simon & Alouini, 2005). However, these fading models are not widely used in the context of performance analysis of digital communication over fading channels due to their rather complicated mathematical expressions. The use of the gamma distribution as an alternative to the log-normal distribution, leads to other, mathematically more tractable, composite distributions such as the generalized-K (K_G) distribution which is a mixture of a Nakagami-m and a gamma distribution (Bithas et al., 2006; Peppas, 2009). Moreover, it has been proved that this alternative model has both theoretical and experimental support (Abdi & Kaveh, 1999; 2000). Furthermore, the K_G distribution includes the well known Double-Rayleigh model (Uysal, 2006). Therefore, it can be further employed to model the power statistics in so-called cascaded multi-path fading channels. Such channels occur in propagation through keyholes or in serial relaying communications systems employing fixed gain relays (Peppas et al., 2010; Yilmaz & Alouini, 2009). Consequently, the K_G distribution can accurately capture the effects of the combined multi-path fading and shadowing or cascaded multi-path fading, which are both frequently encountered in wireless systems. The squared K_G distribution, also known as the gamma-gamma distribution in optical communications theory, has been recently used in the performance analysis of free-space optical (FSO) communications systems over atmospheric turbulence channels (Al-Habash et al., 2001; Bayaki et al., 2009; Uysal et al., 2006). In FSO communications, the atmospheric turbulence results in rapid fluctuations at

the received signal that severely degrade the optical link's performance. The gamma-gamma model in wireless optical communications theory is based on the assumption that small-scale irradiance fluctuations are modulated by large-scale irradiance fluctuations of the propagating wave, both modeled as independent gamma distributions. This distribution has become the dominant fading channel model for FSO links due to its excellent agreement with measurement data for a wide range of turbulence conditions (Al-Habash et al., 2001; Bayaki et al., 2009).

A closed form expression for the K_G PDF is obtained as follows: Let R be the instantaneous amplitude of a flat fading channel with PDF modeled by the Nakagami-m distribution, i.e.

$$f_{R|Y}(r) = \frac{2m^m r^{2m-1}}{Y^m \Gamma(m)} \exp\left(-\frac{mr^2}{Y}\right), r \geq 0 \tag{33}$$

When multi-path fading is superimposed on shadowing, the parameter Y, randomly varies, modeled in the following analysis with the gamma distribution. The PDF of Y is given by:

$$f_Y(y) = \frac{k^k y^{k-1} \exp(-ky/\Omega)}{\Gamma(k)\Omega^k}, y \geq 0 \tag{34}$$

where k is the shaping parameter and $\Omega = \mathbb{E}\langle Y \rangle$. The PDF of the K_G distribution, $f_R(r)$, is obtained by averaging (33) over (34), i.e.

$$f_R(r) = \int_0^\infty f_{R|Y}(r|y) f_Y(y) dy \tag{35}$$

Using (Gradshteyn & Ryzhik, 2000b, Eq. (3.471/9)) the analytical expression for the PDF of the corresponding fading envelope R is obtained as

$$f_R(r|m,k,\Omega) = \frac{4\Psi^{k+m}}{\Gamma(m)\Gamma(k)} r^{k+m-1} K_{k-m}(2\Psi r), \ r \geq 0 \tag{36}$$

where $K_a(\cdot)$ is the modified Bessel function of the second kind and order a and $\Psi = \sqrt{\frac{km}{\Omega}}$. For $k \to \infty$, (36) approximates the Nakagami-m distribution; for $m = 1$, it approximately models Rayleigh-lognormal fading conditions (Bithas et al., 2006); while for $m \to \infty$ and $k \to \infty$, it approaches the additive white Gaussian noise (AWGN) channel. The PDF of the average SNR per symbol, γ is given by

$$f_\gamma(\gamma) = \frac{2\Xi^{k+m}}{\Gamma(m)\Gamma(k)} \gamma^{(k+m)/2-1} K_{k-m}(2\Xi\sqrt{w}) \tag{37}$$

where $\Xi = \sqrt{\frac{km}{\bar{\gamma}}}$. The MGF of γ, can be obtained using (Bithas et al., 2006, Eq. (4)) as

$$\mathcal{M}_\gamma(s) = \left(\frac{\Xi^2}{s}\right)^{(k+m-1)/2} \exp\left(\frac{\Xi^2}{2s}\right) W_{-(k+m-1)/2,(k-m)/2}\left(\frac{\Xi^2}{s}\right) \tag{38}$$

where $W_{\lambda,\mu}(\cdot)$ is the Whittaker function (Gradshteyn & Ryzhik, 2000a, Eq. (9.220)).

4. Performance metrics of fading channels

4.1 Channel capacity

The huge growth of the number of the mobile subscribers world-wide, during the last decade, together with the increasing demand for higher information transmission rates and flexible access to diverse services, has raised demand for spectral efficiency in wireless communications systems. The pioneering work of Shannon established the significance of channel capacity as the maximum rate of communication for which arbitrarily small error probability can be achieved. Thus, the Shannon capacity provides a benchmark against which the spectral efficiency of practical transmission strategies can be compared.

Of particular interest is the study of the Shannon capacity of fading channels under different assumptions about transmitter and receiver channel knowledge. Shannon capacity results can be used to compare the effectiveness of both adaptive and nonadaptive transmission strategies in fading channels against their theoretical maximum performance. The main idea behind these transmission schemes is balancing of the link budget in real time, through adaptive variation of the transmitted power level, symbol rate constellation size, coding rate/scheme, or any combination of these parameters (Alouini & Goldsmith, 1999). Such schemes can provide a higher average spectral efficiency without sacrificing error rate performance. The disadvantage of these adaptive techniques is that they require an accurate channel estimate at the transmitter, additional hardware complexity to implement adaptive transmission, and buffering/delay of the input data since the transmission rate varies with channel conditions (Goldsmith & Varaiya, 1997).

Various works available in the open technical literature study the spectral efficiency of adaptive transmission techniques over fading channels. Representative past works can be found in (Alouini & Goldsmith, 1999; Laourine et al., 2008; Mallik et al., 2004; Peppas, 2010). For example in (Alouini & Goldsmith, 1999), an extensive analysis of the Shannon capacity of adaptive transmission techniques in conjunction with diversity combining over Rayleigh fading channels has been presented. Moreover in (Mallik et al., 2004), by assuming maximum ratio combining diversity (MRC) reception under correlated Rayleigh fading, closed-form expressions for the single-user capacity were presented. Finally, in (Laourine et al., 2008) the capacity of generalized-K fading channels under different adaptive transmission techniques was studied in detail.

The adaptive transmission schemes under consideration are optimal simultaneous power and rate adaptation (OPRA), optimal rate adaptation with constant transmit power (ORA), channel inversion with fixed rate (CIFR) and truncated channel inversion with fixed rate (TCIFR)(Biglieri et al., 1998; Goldsmith & Varaiya, 1997; Luo et al., 2003). The ORA scheme achieves the ergodic capacity by using variable-rate transmission relative to the channel conditions while the transmit power remains constant. The OPRA scheme also achieves the ergodic capacity of the system by varying the rate and power relative to the channel conditions, which, however, may not be appropriate for applications requiring a fixed rate. Finally, the CIFR and TCIFR schemes achieve the outage capacity of the system, defined as the maximum constant transmission rate that can be supported under all channel conditions with some outage probability (Biglieri et al., 1998; Luo et al., 2003).

4.1.1 Optimal rate adaptation with constant transmit power

Under the ORA policy, where channel state information (CSI) is available at the receiver only, the capacity is known to be given by (Alouini & Goldsmith, 1999; Lazarakis et al., 1994)

$$\langle C \rangle_{ORA} = \frac{1}{\ln 2} \int_0^\infty f_\gamma(\gamma) \ln(1+\gamma) d\gamma \tag{39}$$

It is noted that $\langle C \rangle_{ORA}$ was introduced by Lee in (Lee, 1990) as the average channel capacity of a flat-fading channel, since it is obtained by averaging the capacity of an AWGN channel $C_{awgn} = \log_2(1+\gamma)$ over the distribution of the received SNR γ. That is why capacity under the ORA scheme is also called ergodic capacity. Using Jensen's inequality we observe that

$$\langle C \rangle_{ORA} = \frac{1}{\ln 2} \mathbb{E} \langle \ln(1+\gamma) \rangle \leq \frac{1}{\ln 2} \ln(1 + \mathbb{E} \langle \gamma \rangle) = \frac{1}{\ln 2} \ln(1+\overline{\gamma}) \tag{40}$$

where $\overline{\gamma}$ is the average SNR on the channel. Therefore we observe that the Shannon capacity under the ORA scheme is less than the Shannon capacity of an AWGN channel with the same average SNR. In other words, fading reduces Shannon capacity when only the receiver has CSI. Moreover, if the receiver CSI is not perfect, capacity can be significantly decreased (Goldsmith, 2005; Lapidoth & Shamai, 1997).

It is worth mentioning here, that the ergodic capacity is a very significant metric for the study of the wireless optical communication links, due to the strong influence of the atmospheric conditions in their performance, see e.g. (Andrews et al., 1999; Gappmair et al., 2010; Garcia-Zambrana, Castillo-Vasquez & Castillo-Vasquez, 2010; Garcia-Zambrana, Castillo-Vazquez & Castillo-Vazquez, 2010; Li & Uysal, 2003; Liu et al., 2010; Nistazakis, Karagianni, Tsigopoulos, Fafalios & Tombras, 2009; Nistazakis, Tombras, Tsigopoulos, Karagianni & Fafalios, 2009; Peppas & Datsikas, 2010; Popoola et al., 2008; Sandalidis & Tsiftsis, 2008; Tsiftsis, 2008; Vetelino et al., 2007; Zhu & Kahn, 2002). More specifically, the fast changes of the atmospheric turbulence conditions fades fast the transmitted signal and as a result, the estimation of the instantaneous channel capacity is nearly meaningless in this area of wireless communications.

4.1.2 Optimal simultaneous power and rate adaptation

For optimal power and rate adaptation (OPRA), the capacity is known to be given by (Alouini & Goldsmith, 1999, Eq. (7))

$$\langle C \rangle_{OPRA} = \int_{\gamma_0}^\infty \log_2 \left(\frac{\gamma}{\gamma_0} \right) f_\gamma(\gamma) d\gamma \tag{41}$$

where γ_0 is the optimal cutoff SNR level below which data transmission is suspended. This optimal cutoff SNR must satisfy the equation (Alouini & Goldsmith, 1999, Eq. (8))

$$\int_{\gamma_0}^\infty \left(\frac{1}{\gamma_0} - \frac{1}{\gamma} \right) f_\gamma(\gamma) d\gamma = 1 \tag{42}$$

Since no data is sent when $\gamma < \gamma_0$, the optimal policy suffers a probability of outage P_{out}, equal to the probability of no transmission, given by

$$P_{\text{out}} = 1 - \int_{\gamma_0}^\infty f_\gamma(\gamma) d\gamma \tag{43}$$

4.1.3 Channel inversion with fixed rate

Channel inversion with fixed rate (CIFR) is a suboptimal transmitter adaptation scheme where the transmitter uses the CSI to maintain a constant received power, i.e., it inverts the channel fading. The channel then appears to the encoder and decoder as a time-invariant AWGN channel. CIFR is the least complex technique to implement, assuming good channel estimates are available at the transmitter and receiver. This technique uses fixed-rate modulation and a fixed code design, since the channel after channel inversion appears as a time-invariant AWGN channel. The channel capacity is given by

$$\langle C \rangle_{CIFR} = \frac{1}{\ln 2} \ln \left[1 + \frac{1}{\int_0^\infty \gamma^{-1} f_\gamma(\gamma) \, d\gamma} \right] \tag{44}$$

This technique has the advantage of maintaining a fixed data rate over the channel regardless of channel conditions. Therefore, the channel capacity given in (44) is called zero-outage capacity, since the data rate is fixed under all channel conditions and there is no channel outage. Practical coding techniques are available in the open technical literature that achieve near-capacity data rates on AWGN channels, so the zero-outage capacity can be approximately achieved in practice. It should be stressed that zero-outage capacity can exhibit a large data rate reduction relative to Shannon capacity in extreme fading environments. For example, in Rayleigh fading $\int_0^\infty \gamma^{-1} f_\gamma(\gamma) \, d\gamma$ diverges, and thus the zero-outage capacity given by (44) is zero. Channel inversion is also common in spread spectrum systems with near-far interference imbalances (Goldsmith, 2005).

4.1.4 Truncated channel inversion with fixed rate and outage capacity

The CIFR policy suffers a large capacity penalty relative to the other techniques, since a large amount of the transmitted power is required to compensate for the deep channel fades. By suspending transmission in particularly bad fading states (outage channel states), a higher constant data rate can be maintained in the other states and henceforth a significant increase in capacity. The outage capacity is defined as the maximum data rate that can be maintained in all nonoutage channel states times the probability of nonoutage. Outage capacity is achieved by using a modified inversion policy which inverts the channel fading only above a fixed cutoff fade depth γ_0, which we shall refer to as TCIFR. The capacity with this truncated channel inversion and fixed rate policy is given by

$$\langle C \rangle_{TCIFR} = \frac{1}{\ln 2} \ln \left[1 + \frac{1}{\int_{\gamma_0}^\infty \gamma^{-1} f_\gamma(\gamma) \, d\gamma} \right] (1 - P_{out}(\gamma_0)) \tag{45}$$

where P_{out} is the outage probability given by (43).

4.2 Outage probability

The outage probability is an important performance metric of wireless communications systems operating over fading channels. It is defined as the probability that the instantaneous SNR at the receiver output, γ, falls below a predefined outage threshold, γ_{th}. Based on this definition, the outage probability can be mathematically expressed as

$$P_{out} = \Pr\{\gamma < \gamma_{th}\} = \int_0^{\gamma_{th}} f_\gamma(\gamma) \mathrm{d}\gamma = F_\gamma(\gamma_{th}) \tag{46}$$

where $F_\gamma(\cdot)$ is the cumulative distribution of γ. For many of the well known fading distributions, the outage probability can be analytically evaluated using (46). An alternative method to numerically evaluate P_{out} can be obtained using the MGF of γ. More specifically, using the well known Laplace transform property $\mathcal{M}_\gamma(s) = s\mathbb{L}\{F_\gamma(\gamma)\}$, where $\mathbb{L}\{\cdot\}$ denotes Laplace transformation, P_{out} can be obtained as

$$P_{\text{out}} = \mathbb{L}^{-1}\left\{\frac{\mathcal{M}_\gamma(s)}{s}; s; t\right\}\Bigg|_{t=\gamma_{\text{th}}} \tag{47}$$

Consequently, P_{out} can be evaluated using any of the well known methods for the numerical inversion of the Laplace transform, such as the Euler method, presented in (Abate & Whitt, 1995).

4.3 Average bit error probability

The last performance metric we deal with in this chapter, is the average bit error probability (ABEP). This performance metric is one of the most revealing regarding the wireless system behavior and the one most often illustrated in technical documents containing performance evaluation of wireless communications systems (Simon & Alouini, 2005). We present two methods to evaluate ABEP: A PDF-based approach and an MGF-based one.

4.3.1 PDF-based approach

Modulation Scheme	A	B	Λ
BPSK	$1/2$	1	-
BFSK	$1/2$	$1/2$	-
QPSK and MSK	1	$1/2$	-
Square M-QAM	$2\left(1-\frac{1}{\sqrt{M}}\right)$	$\frac{3}{2(M-1)}$	-
NBFSK	$1/2$	$1/2$	-
BDPSK	$1/2$	1	-
$\pi/4$-DQPSK	$\frac{1}{2\pi}$	$\frac{2}{2-\sqrt{2}\cos(\theta)}$	π
M-PSK	$\frac{1}{\pi}$	$\frac{\sin^2(\pi/M)}{\sin^2\theta}$	$\pi\left(1-\frac{1}{M}\right)$
M-DPSK	$\frac{1}{\pi}$	$\frac{\sin^2(\pi/M)}{1+\cos(\pi/M)\cos\theta}$	$\pi\left(1-\frac{1}{M}\right)$

Table 1. Parameters A, B and Λ for various coherent and non-coherent modulation schemes (PDF-based approach)

One common method we can use to determine the error performance of a digital communications system is to evaluate the decision variables and from these to determine the probability of error. For a fixed SNR, γ, analytical expressions for the error probability are well known for a variety of binary and M-ary modulation schemes (see for example (Proakis & Salehi, 2008)). When γ randomly varies, the ABEP can be obtained by averaging the conditional bit error probability, $P_e(E|\gamma)$, over the PDF of γ, namely

$$\overline{P}_{be}(E) = \int_0^\infty P_e(E|\gamma)f_\gamma(\gamma)\mathrm{d}\gamma \tag{48}$$

This yields:

Modulation Scheme	ABEP
BPSK	$\frac{1}{\pi} \int_0^{\pi/2} \mathcal{M}_\gamma \left(\frac{1}{\sin^2 \theta} \right) d\theta$
BFSK	$\frac{1}{\pi} \int_0^{\pi/2} \mathcal{M}_\gamma \left(\frac{1}{2\sin^2 \theta} \right) d\theta$
BFSK with minimum correlation	$\frac{1}{\pi} \int_0^{\pi/2} \mathcal{M}_\gamma \left(\frac{0.715}{\sin^2 \theta} \right) d\theta$
M-AM	$\frac{2(M-1)}{M\pi \log_2(M)} \int_0^{\pi/2} \mathcal{M}_\gamma \left(\frac{g_{AM}}{\sin^2 \theta} \right) d\theta, g_{AM} = \frac{3\log_2(M)}{M^2-1}$
Square M-QAM	$\frac{4}{\pi \log_2(M)} \left\{ \left(1 - \frac{1}{\sqrt{M}} \right) \int_0^{\pi/2} \mathcal{M}_\gamma \left(\frac{g_{QAM}}{\sin^2 \theta} \right) d\theta \right.$ $\left. - \left(1 - \frac{1}{\sqrt{M}} \right)^2 \int_0^{\pi/4} \mathcal{M}_\gamma \left(\frac{g_{QAM}}{\sin^2 \theta} \right) d\theta \right\}, \quad g_{QAM} =$ $\frac{3\log_2(M)}{2(M-1)}$
NBFSK	$\frac{1}{2} \mathcal{M}_\gamma \left(\frac{1}{2} \right)$
BDPSK	$\frac{1}{2} \mathcal{M}_\gamma (1)$
M-PSK	$\frac{1}{\pi \log_2(M)} \int_0^{\pi-\pi/M} \mathcal{M}_\gamma \left(\frac{g_{PSK}}{\sin^2 \theta} \right) d\theta, \quad g_{PSK} =$ $\log_2(M) \sin^2 \left(\frac{\pi}{M} \right)$
M-DPSK	$\frac{1}{\pi \log_2(M)} \int_0^{\pi-\pi/M} \mathcal{M}_\gamma \left(\frac{g_{PSK}}{1+\cos(\theta)\cos(\pi/M)} \right) d\theta$

Table 2. Parameters A, B and Λ for various coherent and non-coherent modulation schemes (MGF-based approach)

- For non-coherent binary frequency shift keying (BFSK) and binary differential phase shift keying (BDPSK), $P_e(E|\gamma)$ can be expressed as

$$P_e(E|\gamma) = A \exp(-B\gamma) \tag{49}$$

  where A,B constants depending on the specific modulation scheme.

- For binary phase shift keying (BPSK), square M-ary Quadrature Amplitude Modulation (M-QAM) and for high values of the average input SNR, $P_e(E|\gamma)$ is of the form

$$P_e(E|\gamma) = A \text{erfc}(\sqrt{B\gamma}) \tag{50}$$

  where $\text{erfc}(\cdot)$ denotes the complementary error function (Gradshteyn & Ryzhik, 2000a, Eq. (8.250/1)).

- Finally, for Gray encoded $\pi/4$- Differential Quadrature Phase-Shift Keying ($\pi/4$-DQPSK), M-ary Phase-Shift Keying (M-PSK) and M-ary Differential Phase-Shift Keying (M-DPSK), $P_e(E|\gamma)$ is expressed as

$$P_e(E|\gamma) = \int_0^\Lambda \exp[-B(\theta)\gamma]d\theta \tag{51}$$

The values of A, B and Λ for different modulation schemes are summarized in Table 1.

4.3.2 MGF-based approach
The MGF-based approach is useful in simplifying the mathematical analysis required for the evaluation of the average bit error probability and allows unification under a common framework in a large variety of digital communication systems, covering virtually all known modulation and detection techniques and practical fading channel models (Simon & Alouini, 2005). Using the MGF-based approach, the ABEP for non-coherent binary modulation

signallings can be directly calculated (e.g. for BDPSK, $\overline{P}_{be}(E) = 0.5\mathcal{M}(1)$. For other types of modulation formats, such as M-PSK and M-QAM, single integrals with finite limits and integrands composed of elementary (exponential and trigonometric) functions have to be readily evaluated via numerical integration. Various ABEP expressions, evaluated using the MGF approach are presented in Table 2. For high-order modulation schemes, Gray coding is assumed.

5. References

Aalo, V., T.Piboongungon & Iskander, C.-D. (2005). Bit-error rate of binary digital modulation schemes in generalized gamma fading channels, *IEEE Communications Letters* 9(2): 139–141.

Abate, J. & Whitt, W. (1995). Numerical Inversion of Laplace Transforms of Probability Distributions, *ORSA Journal on Computing* 1(7): 36–43.

Abdi, A. & Kaveh, M. (1999). On the utility of the gamma PDF in modeling shadow fading (slow fading), *Proceedings of IEEE Vehicular Technology Conference*, Houston, TX, pp. 2308–2312.

Abdi, A. & Kaveh, M. (2000). Comparison of DPSK and MSK Bit Error Rates for K and Rayleigh-Lognormal Fading Distributions, *IEEE Commnunications Letters* 4(4): 122–124.

Abramovitz, M. & Stegun, I. (1964). *Handbook of Mathematical Functions with Formulas, Graphs, and Mathematical Tables*, Dover, New York.

Al-Habash, M. A., Andrews, L. C. & Phillips, R. L. (2001). Mathematical model for the irradiance PDF of a laser beam propagating through turbulent media, *Optical Engineering* 40(8): 1554–1562.

Alouini, M. S. & Goldsmith, A. J. (1999). Capacity of rayleigh fading channels under different adaptive transmission and diversity-combining techniques, *IEEE Transactions on Vehicular Technology* 48(4): 1165–1181.

Andrews, L. C., Phillips, R. L., Hopen, C. Y. & Al-Habash, M. A. (1999). Theory of optical scintillation, *Journal of Optical Society of America A* 16: 1417–1429.

Aulin, T. (1981). Characteristics of a digital mobile radio channel, *IEEE Transactions on Vehicular Technology* 30: 45–53.

Basu, S., MacKenzie, E. M., Basu, S., Costa, E., Fougere, P. F., Carlson, H. C. & Whitney, H. E. (1987). 250 MHz/GHz scintillation parameters in the equatorial, polar, and aural environments, *IEEE Journal on Selected Areas in Communications* 5: 102–115.

Bayaki, E., Schober, R. & Mallik, R. (2009). Performance analysis of MIMO free-space optical systems in gamma-gamma fading, *IEEE Transaction on Communications* 57(11): 3415–3424.

Belmonte, A. & Kahn, J. M. (2009). Capacity of coherent free space optical links using atmospheric compensation techniques, *Optics Express* 17(4): 2763–2773.

Bertoni, H. (1988). Coverage prediction for mobile radio systems operating in the 800 / 900 MHz frequency rangeÜreceived signal fading distributions, *IEEE Transactions on Vehicular Technology* 37(1): 57–60.

Biglieri, E., Proakis, J. & Shamai, S. (1998). Fading channels: Information theoretic and communications aspects, *IEEE Transactions on Information Theory* 44: 2619–2692.

Bischoff, K. & Chytil, B. (1969). A note on scintillation indices, *Planetary and Space Science* 17: 1059–1066.

Bithas, P. S., Sagias, N. C., Mathiopoulos, P. T., Karagiannidis, G. K. & Rontogiannis, A. A. (2006). On the performance analysis of digital comminications over generalized-*K* fading channels, *IEEE Communications Letters* 10(5): 353–355.

Braun, W. R. & Dersch, U. (1991). A physical mobile radio channel model, *IEEE Transactions on Vehicular Technology* 40(2): 472–482.

Bultitude, R. J. C., Mahmoud, S. A. & Sullivan, W. A. (1989). A comparison of indoor radio propagation characteristics at 910 MHz and 1.75 GHz, *IEEE Journal on Selected Areas in Communications* 7: 20–30.

Chytil, B. (1967). The distribution of amplitude scintillation and the conversion of scintillation indices, *Journal of Atmospheric and Solar-Terrestrial Physics* 29: 1175–1177.

Cook, I. D. (1981). *The H-function and probability density functions of certain algebraic combinations of independent random variables with H-function probability distribution*, PhD thesis, The University of Texas at Austin, Austin, TX.

Ermolova, N. (2008). Moment Generating Functions of the Generalized $\eta - \mu$ and $k - \mu$ Distributions and Their Applications to Performance Evaluations of Communication Systems, *IEEE Communications Letters* 12(7): 502 – 504.

Filho, J. C. S. S. & Yacoub, M. D. (2005). Highly accurate η-μ approximation to sum of *m* independent non-identical hoyt variates, *IEEE Antenna and Propagation Letters* 4: 436–438.

Gappmair, W., Hranilovic, S. & Leitgeb, E. (2010). Performance of ppm on terrestrial fso links with turbulence and pointing errors, *IEEE Communications Letters* 14(5): 468–470.

Garcia-Zambrana, A., Castillo-Vasquez, C. & Castillo-Vasquez, B. (2010). On the capacity of fso links over gamma gamma atmospheric turbulence channels using ook signaling, *Eurasip Journal on Wireless Communications and Networking, art. no. 127657, pages 9* .

Garcia-Zambrana, A., Castillo-Vazquez, B. & Castillo-Vazquez, C. (2010). Average capacity of fso links with transmit laser selection using non-uniform ook signaling over exponential atmospheric turbulence channels, *Optics Express* 18(19): 20445–20454.

Goldsmith, A. (2005). *Wireless Communications*, Cambridge University Press.

Goldsmith, A. J. & Varaiya, P. P. (1997). Capacity of fading channels with channel side information, *IEEE Transactions on Information Theory* 43(6): 1986–1992.

Gradshteyn, I. & Ryzhik, I. M. (2000a). *Tables of Integrals, Series, and Products*, 6 edn, Academic Press, New York.

Gradshteyn, I. S. & Ryzhik, I. M. (2000b). *Table of Integrals, Series, and Products*, 6 edn, ed. New York: Academic.

Hashemi, H. (1993). The indoor radio propagation channel, *Proceedings of the IEEE* 81(7): 943–967.

Hoyt, R. S. (1947). Probability functions for the modulus and angle of the normal complex variate, *Bell System Technical Journal* 26: 318–359.

James, H. B. & Wells, P. I. (1955). Some tropospheric scatter propagation measurements near the radio-horizon, *Proceedings of the IRE* pp. 1336–1340.

Kamalakis, T., Sphicopoulos, T., Muhammad, S. & Leitgeb, E. (2006). Estimation of the power scintillation probability density function in free-space optical links by use of multicanonical monte carlo sampling, *Optics Letters* 31(21): 3077–3079.

Karagiannidis, G., Zogas, D., Sagias, N., Kotsopoulos, S. & Tombras, G. (2005). Equal-gain and maximal-ratio combining over nonidentical Weibull fading channels, *IEEE Transactions on Wireless Communications* 4(3): 841–846.

Katsis, A., Nistazakis, H. E. & Tombras, G. S. (2009). Bayesian and frequentist estimation of the performance of free space optical channels under weak turbulence conditions, *Journal of the Franklin Institute* 346: 315–327.

Laourine, A., Alouini, M. S., Affes, S. & Stephenne, A. (2008). On the capacity of Generalized-K fading channels, *IEEE Transactions on Wireless Communications* 7(7): 2441–2445.

Laourine, A., Stephenne, A. & Affes, S. (2007). Estimating the ergodic capacity of log-normal channels, *IEEE communication Letters* 11(7): 568–570.

Lapidoth, A. & Shamai, S. (1997). Fading channels: how perfect need "perfect side information" be?, *IEEE Transactions on Information Theory* pp. 1118–1134.

Lazarakis, F., Tombras, G. S. & Dangakis, K. (1994). Average channel capacity in a mobile radio environment with rician statistics, *IEICE Trans. Commun.* E77-B(7): 971–977.

Lee, W. C. Y. (1990). Estimate of channel capacity in Rayleigh fading environment, *IEEE Transactions on Vehicular Technology* 39: 187–190.

Li, J. T. & Uysal, M. (2003). Optical wireless communications: system model, capacity and coding, *Proc. Vehic. Tech. Conf.* pp. 168–172.

Liu, C., Yao, Y., Sun, Y., Xiao, J. & Zhao, X. (2010). Average capacity optimization in free-space optical communication system over atmospheric turbulence channels with pointing errors, *Optics Letters* 35(19): 3171–3173.

Luo, J., Lin, L., Yates, R. & Spasojevic, P. (2003). Service outage based power and rate allocation, *IEEE Transactions on Information Theory* 49: 323–330.

Majumdar, A. K. (2005). Free-space laser communications performance in the atmospheric channel, *Journal of optical and fiber communications research* 2: 345–396.

Mallik, R. K., Win, M. Z., Shao, J. W., Alouini, M.-S. & Goldsmith, A. J. (2004). Channel Capacity of Adaptive Transmission With Maximal Ratio Combining in Correlated Rayleigh Fading, *IEEE Transactions on Wireless Communications* 3(4): 1124–1133.

Munro, G. H. (1963). Scintillation of radio signals from satellites, *Journal of Geophysical Research* 68.

Nakagami, M. (1960). The *m*-distribution: A general formula of intensity distribution of rapid fading, *Statistical Methods in Radio Wave Propagation*, Pergamon Press, Oxford, U.K., pp. 3–36.

Nistazakis, H. E., Karagianni, E. A., Tsigopoulos, A. D., Fafalios, M. E. & Tombras, G. S. (2009). Average capacity of optical wireless communication systems over atmospheric turbulence channels, *Journal of Lightwave Technology* 27(8): 974–979.

Nistazakis, H. E., Tombras, G. S., Tsigopoulos, A. D., Karagianni, E. A. & Fafalios, M. E. (2009). Capacity estimation of optical wireless communication systems over moderate to strong turbulence channels, *Journal of Communications and Networks* 11(4): 387–392.

Nistazakis, H. E., Tsiftsis, T. A. & Tombras, G. S. (2009). Performance analysis of free-space optical communication systems over atmospheric turbulence channels, *IET Communications* 3(8): 1402–1409.

Peppas, K. (2009). Performance evaluation of triple-branch GSC diversity receivers over generalized-K fading channels, *IEEE Communications Letters* 13(11): 829–831.

Peppas, K., Lazarakis, F., Alexandridis, A. & Dangakis, K. (2009). Error performance of digital modulation schemes with MRC diversity reception over η-μ fading channels, *IEEE Transactions on Wireless Communications* 8(10): 4974–4980.

Peppas, K., Lazarakis, F., Alexandridis, A. & Dangakis, K. (2010). Cascaded generalised-k fading channel, *IET Communications* 4(1): 116–124.

Peppas, K. P. (2010). Capacity of η-μ fading channels under different adaptive transmission techniques, *IET Communnications* 4: 532–539.

Peppas, K. P. & Datsikas, C. K. (2010). Average symbol error probability of general-order rectangular quadrature amplitude modulation of optical wireless communication systems over atmospheric turbulence channels, *IEEE/OSA Journal of Optical Communications and Networking* 2(1-3): 102–110.

Popoola, W. O., Ghassemlooy, Z. & Ahmadi, V. (2008). Performance of sub-carrier modulated free space optical communication link in negative exponential turbulence environment, *International Journal of Autonomous and Adaptive Communication Systems* 1(3): 342–355.

Proakis, J. & Salehi, M. (2008). *Digital Communications*, McGraw-Hill.

Prudnikov, A. P., Brychkov, Y. A. & Marichev, O. I. (1986). *Integrals and Series Volume 3: More Special Functions*, 1 edn, Gordon and Breach Science Publishers.

Rappaport, T. S. & McGillem, C. D. (1989). UHF fading in factories, *IEEE Journal on Selected Areas in Communications* 7: 40–48.

Rice, S. O. (1948). Statistical properties of a sine wave plus random noise, *Bell System Technical Journal* 27: 109–157.

Sagias, N. C. & Karagiannidis, G. K. (2005). Gaussian class multivariate weibull distributions: theory and applications in fading channels, *IEEE Transactions on Information Theory* 51(10): 3608–3619.

Sagias, N. C. & Mathiopoulos, P. T. (2005). Switched diversity receivers over generalized gamma fading channels, *IEEE Communications Letters* 9(10): 871–873.

Sagias, N., Karagiannidis, G. & Tombras, G. (2004). Error-rate analysis of switched diversity receivers in Weibull fading, *Electronics Letters* 40(11): 681–682.

Sagias, N., Karagiannidis, G., Zogas, D., Mathiopoulos, P. & Tombras, G. (2004). Performance analysis of dual selection diversity in correlated Weibull fading channels, *IEEE Transactions on Communications* 52(7): 1063–1067.

Sagias, N., Mathiopoulos, P. & Tombras, G. (2003). Selection diversity receivers in Weibull fading: Outage probability and average signal-to-noise ratio, *Electronics Letters* 39(25): 1859–1860.

Sagias, N. & Tombras, G. (2007). On the cascaded weibull fading channel model, *Journal of the Franklin Institute* 344(1): 1–11.

Sagias, N., Zogas, D., Karagiannidis, G. & Tombras, G. (2004). Channel capacity and second-order statistics in Weibull fading, *IEEE Communications Letters* 8(6): 377–379.

Sandalidis, H. G. & Tsiftsis, T. A. (2008). Outage probability and ergodic capacity of free-space optical links over strong turbulence, *Electronics Letters* 44(1): 46–47.

Shaft, P. D. (1974). On the relationship between scintillation index and Rician fading, *IEEE Transactions on Communications* 22: 731–732.

Simon, M. K. & Alouini, M. S. (2005). *Digital Communication over Fading Channels*, Wiley.

Stacy, E. (1962). A generalization of the gamma distribution, *The Annals of Mathematical Statistics* 3(33): 1187–1192.

Staley, T. L., North, R. C., Ku, W. H. & Zeidler, J. R. (1996). Performance of coherent MPSK on frequency selective slowly fading channels, *Proceedings of IEEE Vehicular Technology Conference (VTC 96)*, Atlanta, pp. 784–788.

Stein, S. (1987). Fading channel issues in system engineering, *IEEE Journal on Selected Areas in Communications* 5(2): 68–69.

Sugar, G. R. (1955). Some fading characteristics of regular VHF ionospheric propagation, *Proceedings of the IRE* pp. 1432–1436.

Tse, D. & Viswanath, P. (2005). *Fundamentals of Wireless Communication*, Cambridge University Press.

Tsiftsis, T. A. (2008). Performance of heterodyne wireless optical communication systems over gamma-gamma atmospheric turbulence channels, *Electronics Letters* 44: 373–375.

Uysal, M. (2006). Diversity analysis of space-time coding in cascaded rayleigh fading channels, *IEEE Commnunications Letters* 10(3): 165–167.

Uysal, M., Li, J. T. & Yu, M. (2006). Error rate performance analysis of coded free-space optical links over gamma-gamma atmospheric turbulence channels, *IEEE Transaction on Wireless Communications* 5(6): 1229–1233.

Vetelino, F. S., Young, S. & Andrews, L. (2007). Fade statistics and aperture averaging for gaussian beam waves in moderate to strong turbulence, *Applied Optics* 46(18): 3780–3789.

Yacoub, M. D. (2007a). The α-μ distribution: A physical fading model for the stacy distribution, *IEEE Transactions on Vehicular Technology* 56(1): 27–34.

Yacoub, M. D. (2007b). The κ-μ and the η-μ distribution, *IEEE Antennas and Propagations Magazine* 49(1): 68–81.

Yilmaz, F. & Alouini, M.-S. (2009). Product of the powers of generalized nakagami-m variates and performance of cascaded fading channels, *Proceedings of IEEE Global Telecommunications Conference*, pp. 1–8.

Zhu, X. & Kahn, J. M. (2002). Free-space optical communications through atmospheric turbulence channels, *IEEE Transaction on Communications* 50(8): 1293–1300.

Zogas, D., Sagias, N., Tombras, G. & Karagiannidis, G. (2005). Average output snr of equal-gain diversity receivers over correlative weibull fading channels, *European Transactions on Telecommunications* 16(6): 521–525.
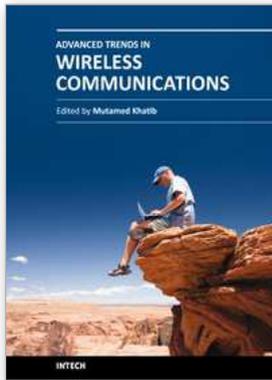
Advanced Trends in Wireless Communications

Edited by Dr. Mutamed Khatib

ISBN 978-953-307-183-1

Hard cover, 520 pages

Publisher InTech

Published online 17, February, 2011

Published in print edition February, 2011

Physical limitations on wireless communication channels impose huge challenges to reliable communication. Bandwidth limitations, propagation loss, noise and interference make the wireless channel a narrow pipe that does not readily accommodate rapid flow of data. Thus, researches aim to design systems that are suitable to operate in such channels, in order to have high performance quality of service. Also, the mobility of the communication systems requires further investigations to reduce the complexity and the power consumption of the receiver. This book aims to provide highlights of the current research in the field of wireless communications. The subjects discussed are very valuable to communication researchers rather than researchers in the wireless related areas. The book chapters cover a wide range of wireless communication topics.

How to reference

In order to correctly reference this scholarly work, feel free to copy and paste the following:

K.P. Peppas, H.E. Nistazakis and G.S. Tombras (2011). An Overview of the Physical Insight and the Various Performance Metrics of Fading Channels in Wireless Communication Systems, Advanced Trends in Wireless Communications, Dr. Mutamed Khatib (Ed.), ISBN: 978-953-307-183-1, InTech, Available from: http://www.intechopen.com/books/advanced-trends-in-wireless-communications/an-overview-of-the-physical-insight-and-the-various-performance-metrics-of-fading-channels-in-wirele